

## CFD-DEM simulations of mixing in dense and dilute flows

Balázs Füvesi<sup>1,\*</sup>, Behrad Esgandari<sup>2,\*\*</sup>, Simon Schneiderbauer<sup>2</sup>, Vanessa Magnanimo<sup>3</sup>, and Stefan Luding<sup>1</sup>

<sup>1</sup>Multi-Scale Mechanics (MSM), Thermal and Fluid Engineering, Faculty of Engineering Technology, University of Twente

<sup>2</sup>Department of Particulate Flow Modelling, Johannes Kepler University

<sup>3</sup>Soil MicroMechanics (SMM), Civil Engineering and Management, Faculty of Engineering Technology, University of Twente

**Abstract.** The mixing of granular materials is important in many industrial applications. Spout fluidized beds enhance particle mixing while operating at lower flow rates than conventional fluidized beds. This study employs CFD-DEM simulations to compare mixing across different regimes of single-, double-, and triple-spout fluidized beds. We compare the averaged solid volume fraction and velocity fields and analyse particle mixing using a collection of mixing indices. Our results indicate that distance-based mixing indices provide clearer insights into mixing dynamics than grid- or contact-based methods. Mixing performance generally improves with increasing bed dynamics. Additionally, vertical mixing is found to be effective due to the dominant circulation patterns in the bed.

### 1 Introduction

Spout fluidized beds combine the benefits of fluidized and spouted beds, enhancing particle circulation and mixing while needing less flow to fluidize particles. These advantages make them suitable for processes like gasification, chemical looping combustion, and pyrolysis [1].

One of the most popular modelling approaches used to simulate spout fluidized beds is computational fluid dynamics coupled with discrete element method (CFD-DEM), where the fluid phase is described by an Eulerian and particles by a Lagrangian framework [2, 3]. Compared to continuum models like the two-fluid model (TFM), CFD-DEM is computationally expensive, but it offers unique information about each particle's trajectory (translational and rotational).

In addition to modelling studies, spout fluidized beds have been investigated experimentally. For instance, Link et al. [4] extracted a flow regime map for a 3D single-spout fluidized bed measuring the pressure drop fluctuations. Their flow regime map is based on the dimensionless parameters  $u_{sp}/u_{mf}$  and  $u_{bg}/u_{mf}$ , representing the spout and background gas velocities normalized by the minimum fluidization velocity.

In another study, van Buijtenen et al. [5] proposed a regime map for triple-spout fluidized beds based on pressure fluctuation measurements and visual observation. In these beds the flow regime can be determined by the interaction between the spouts, which is controlled by dimensionless parameters  $u_{sp}/u_{mf}$  and  $u_{bg}/u_{mf}$ .

The particle information available from CFD-DEM simulations can be adopted to evaluate the particle circulation time [6] and mixing of the particles in spout flu-

idized beds [3]. For instance, Hoorijani et al. [3] quantified the mixing in three flow regimes of a single-spout fluidized bed, including jet-in-fluidized bed, spouting-with-aeration, and intermediate/spout-fluidization using the Lacey index. They found that the mixing rate is higher in jet-in-fluidization and spouting-with-aeration regimes. To date, to our knowledge no modelling study has quantitatively analysed mixing behaviour across different double- and triple-spout fluidized bed regimes. This study compares different flow regimes, the spout fluidized beds' solids volume fraction and flow velocity, and mixing via three indices: Lacey index, contact number ratio and nearest neighbour method.

### 2 Simulation setup

The details of the CFD-DEM equations are provided in [2], and validated against the experimental data of van Buijtenen et al. [5] for the cases S2, D2, and T3 [2]. The Geldart D particles used in the simulations have a diameter of 0.003 m and a density of 2505 kg m<sup>-3</sup>, with other particle properties provided in [2]. A grid spacing of 0.005 m was adopted in the simulations. The details of the single- and multiple-spout fluidized bed geometries (bed height, width, depth),  $u_{bg}$ ,  $u_{sp}$ , and number of particles ( $N_p$ ) are summarized in Table 1. In the case of single-spout fluidized bed, the three regimes are: intermediate (S1), spout-fluidization (S2), and jet-in-fluidized-bed (S3). In the case of double-spout fluidized bed, the three regimes are: multiple-spouts (D1), multiple-interacting-spouts (D2), and multiple-jets-in-fluidized-bed (D3). In the case of triple-spout fluidized bed, the five regimes are: multiple-spouts (T1), multiple-interacting-spouts (T2), multiple-jets-in-fluidized-bed (T3), alternating-two-spout-

\*e-mail: b.fuvesi@utwente.nl

\*\*e-mail: behrad.esgandari@jku.at

contraction (T4), and contracted-spouts-with-periodic-channel-blocking (T5).

**Table 1.** Geometrical and simulation details of the beds.

Name	S1	S2	S3	D1	D2	D3	T1	T2	T3	T4	T5	
Height [mm]	500			900			1800					
Width [mm]	145			290			435					
Depth [mm]	20											
$u_{bg}$ [m/s]	1.2	2.4	3.6	1.2	2.4	3.6	1.2	2.3	4.56	0.23	2.3	
$u_{sp}$ [m/s]	43.5			40.5			43.8					87
$N_p$ [-]	12000			48000			107000					
Spouts [-]	1			2			3					

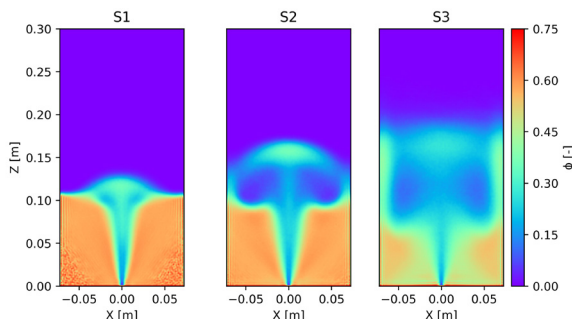
### 3 Comparison of the spout fluidized beds

Before comparing the mixing behaviour of the regimes in single-, double-, and triple- spout fluidized beds, we first compare their continuous flow fields to get a better understanding of their flow pattern and dynamic behaviour.

#### 3.1 Continuous flow fields

To obtain the continuous fields of solid volume fraction ( $\phi$ ) and the solid velocity magnitude ( $v$ ), we use the discrete to continuum mapping of MercuryCG [7]. We use spatial averaging along the depth, and temporal averaging after the steady state is reached. We compare  $\phi$  and  $v$  fields of the regimes in the three spout fluidized beds.

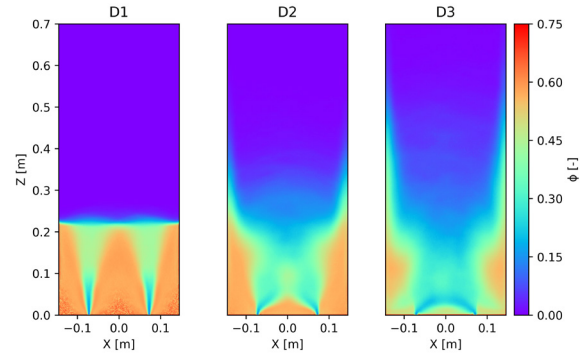
Figure 1 shows  $\phi$  in the three regimes of the single spout fluidized bed. The bed height increases and the regimes become more diluted as  $u_{bg}$  increases from S1 to S3 (see Table 1). In regime S1,  $\phi$  is low in the centre and above 0.5 elsewhere, which indicates that only the centre of the bed is fluidized. The patterns at the corners ( $\phi \geq 0.7$ ) indicate two dead zones where the particles stagnate. In regime S2, there are no such artifacts. However, the bed is still denser at the corners. In regime S3, the corners also become more diluted, with  $\phi$  being around 0.4.



**Figure 1.** Solid volume fraction ( $\phi$ ) in the single-spout regimes.

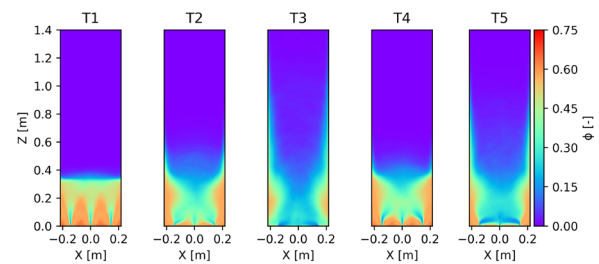
Figure 2 shows  $\phi$  in the three regimes of the double-spout fluidized bed. The bed height increases and the bed becomes more diluted, especially the centre section, as  $u_{bg}$  increases from D1 to D3. In regime D1, the shapes of the two spouts are distinct, with  $\phi$  being low only above the

spouts. Artifacts are still indicating dead zones in the corners and between the two spouts, but their size is smaller compared to S1. In regimes D2 and D3, the bed is more dilute,  $\phi$  is higher along the side walls. In regime D2,  $\phi$  is higher at the centre bottom, whereas in regime D3 it is low, but still around 0.5 at the walls. This indicates that the spouts are increasingly interacting in regimes D2 and D3.



**Figure 2.** Solid volume fraction ( $\phi$ ) in the double-spout regimes.

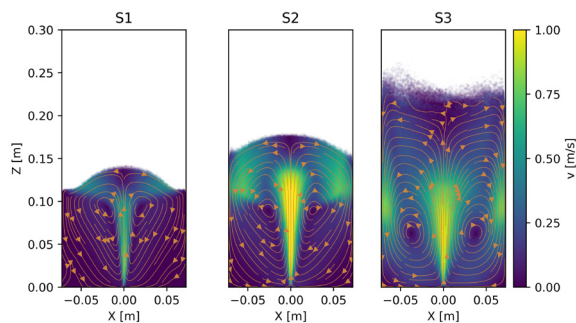
Figure 3 shows  $\phi$  in the five regimes of the triple-spout fluidized bed. As before, with increasing  $u_{bg}$ , the bed becomes more diluted. Regimes T2, T3, and T5, become increasingly dilute in the centre with  $\phi$  higher along the side walls. In regime T1, the shape of the three spouts are distinct with  $\phi$  being low only above the spouts and  $\phi \geq 0.7$  indicating stagnant zones between them. Smaller stagnant zones are also observable in regime T4.



**Figure 3.** Solid volume fraction ( $\phi$ ) in the triple-spout regimes.

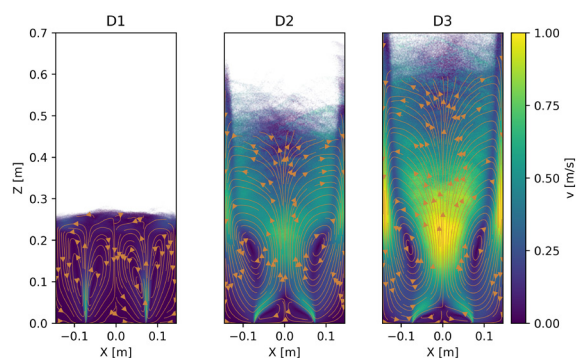
Figure 4 shows  $v$  with streamlines in the three regimes of the single-spout fluidized bed. In regime S1, the velocity at the centre of the bed is moderate, the corner zones have practically zero velocity. In regime S2, the velocity at the centre is higher, the area of stagnant zones is decreased. A clear circulating pattern is formed with particles falling back at the sides of the top portion of the bed. In regime S3, the circulating pattern is intensified with higher  $v$  in most of the bed. Particles are moving downward along the side walls as part of the overall circulation.

Figure 5 shows  $v$  with streamlines in the three regimes of the double-spout fluidized bed. In regime D1, the velocity above the two spouts is moderate, and close to zero



**Figure 4.** Solid velocity magnitude ( $v$ ) with streamlines in the single-spout regimes.

in the corners and between the two spouts. Four weak circulating patterns are formed on both sides of the two spouts. In regimes D2 and D3, the velocities are higher, and with interacting spouts two clear circulating patterns are formed, with higher  $v$  for D3.



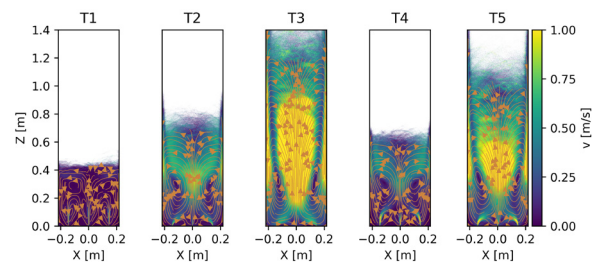
**Figure 5.** Solid velocity magnitude ( $v$ ) with streamlines in the double-spout regimes.

Figure 6 shows  $v$  with streamlines in the five regimes of the triple-spout fluidized bed. In regime T1,  $v$  above the spouts is moderate. Some circulating patterns are present but not clearly developed. In regimes T2 and T4, the velocities are larger and circulating patterns are formed. In regimes T3 and T5, with even higher velocities and interacting spouts, clear circulating patterns are formed. Particles are moving rapidly upward in the centre and downward along the side walls as part of the circulation.

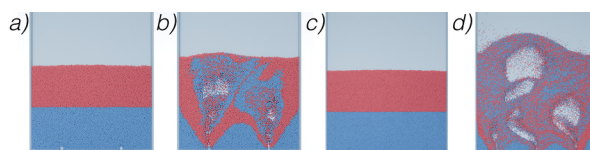
### 3.2 Mixing behaviour

To compare the mixing behaviour of the regimes in vertical direction (see Figure 7) we evaluated a collection of 17 mixing indices but highlight only a few representative examples. For a detailed description of these indices refer to our previous article [8]. We show one mixing index from grid-, contact-, and distance-based methods evaluated in each regime with vertical mixing.

Figure 8 shows the Lacey index, a grid-based mixing index, evaluated in each regime of the spout fluidized

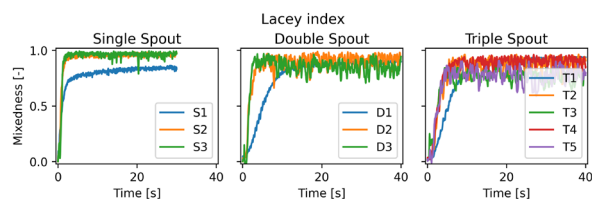


**Figure 6.** Solid velocity magnitude ( $v$ ) with streamlines in the triple-spout regimes.



**Figure 7.** Snapshots of the mixing process in the spout fluidized beds: in regime D1 (a) at the initial state and (b) after 5 s; in regime T4 (c) at the initial state and (d) after 5 s.

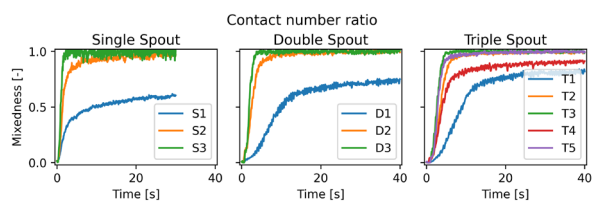
beds. The mixing curves show some general trends between the regimes, with some stagnant zones (S1, D1, and T1). However, they become very noisy in the more dynamic regimes (e.g. D2, D3, T2 and above). This aligns with the recommendation that the Lacey index is not well suited for mixing evaluation in such loose systems as fluidized beds, with the main reason being that the lowest density cells in the inhomogeneous solid fraction in the grids creates artefacts in the cell statistics [8].



**Figure 8.** Mixing evaluated with Lacey index in each regime of the three-spout fluidized beds.

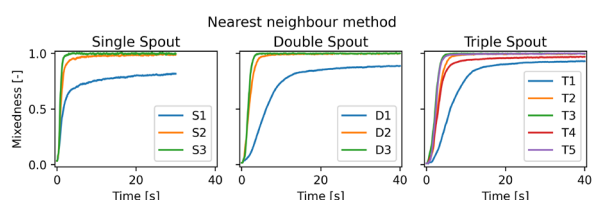
Figure 9 shows the contact number ratio, a contact-based mixing index, evaluated in each regime of the spout fluidized beds. The mixing curves are less noisy compared to Figure 8 and differences become visible between the regimes. However the more dynamic regimes with fewer particles (e.g. S1, S2) still have significant noise. Therefore contact-based indices are still not ideal for mixing evaluation in this system, which can be explained mainly by too little contacts between particles in the loosely packed regions [8].

Figure 10 shows the nearest neighbour method, a distance-based mixing index, evaluated in each regime of the spout fluidized beds. These curves provide a clear insight due to less noise, as distance-based methods are



**Figure 9.** Mixing evaluated with contact number ratio in each regime of the three-spout fluidized beds.

suitable for mixing evaluation in fluidized beds, since they are not sensitive to loosely packed regions [8]. The curve of regimes S1, D1, and T1 converge to values below 0.9 due to the stagnant zones at the corners. This reduces the overall mixedness of the system, since the particles do not move and therefore do not mix in these zones. Regime S3 converges to 1 sooner than S2, which corresponds to increased mixing in the more dynamic regime. This aligns well with experimental studies where an improved mixing in the more dynamic regime with increased  $u_{bg}$  was also observed [9]. The trend of the index from S1 through D1 and T1 to T4 means that the stagnant zones relative size compared to the whole system is smaller than in S1. Regimes T2 and T3 show increased mixing with increasing  $u_{bg}$ . The difference between regimes T3 and T5 is minor, signalling that higher  $u_{sp}$  can also increase mixing when  $u_{bg}$  is lower.



**Figure 10.** Mixing evaluated with nearest neighbour method in each regime of the three-spout fluidized beds.

## 4 Conclusion and outlook

Spout fluidized beds are effective for particle mixing, with the mixing behaviour influenced by the dynamics of the bed. Our analysis highlights that distance-based mixing indices (e.g. Nearest neighbour method) are suitable for evaluating mixing in fluidized beds, better than grid- and contact-based methods, which have poor statistics in highly dynamic dilute regimes. Mixing performance generally improves with increased bed dynamics, as higher  $u_{bg}$  and  $u_{sp}$  enhance particle circulation. However, beyond a limit, a further increase does not lead to significant improvements in mixing. Additionally, mixing in vertical direction is found to be effective due to the circulation patterns within the bed, which promote rapid particle redistribution along the vertical axis with more limited exchange

in the horizontal direction. Future studies could focus on comparing the mixing indices in 3D spout fluidized beds allowing for upscaling.

## 5 Acknowledgements

This research is part of the project TUSAIL and has received funding from the European Horizon2020 Framework Programme for research, technological development and demonstration under grant agreement ID 955661.

## References

- [1] G. Zhou, W. Zhong, A. Yu, J. Xie, Simulation of coal pressurized pyrolysis process in an industrial-scale spout-fluid bed reactor. *Advanced Powder Technology* **30**, 3135-3145 (2019). <https://doi.org/10.1016/j.apt.2019.09.021>
- [2] B. Esgandari, S. Rauchenzauner, C. Goniva, P. Kieckhefen, S. Schneiderbauer, A comprehensive comparison of Two-Fluid Model, Discrete Element Method and experiments for the simulation of single- and multiple-spout fluidized beds. *Chemical Engineering Science* **267**, 118357-1-118357-23 (2023). <https://doi.org/10.1016/j.ces.2022.118357>
- [3] H. Hoorijani, B. Esgandari, R. Zarghami, R. Sotudeh-Gharebagh, N. Mostoufi, Comparative CFD-DEM study of flow regimes in spout-fluid beds. *Particuology* **85**, 323-334 (2024). <https://doi.org/10.1016/j.partic.2023.07.011>
- [4] J. M. Link, L. A. Cuypers, N. G. Deen, J. A.M. Kuipers, Flow regimes in a spout-fluid bed: A combined experimental and simulation study. *Chemical Engineering Science* **60**, 3425-3442 (2005). <https://doi.org/10.1016/j.ces.2005.01.027>
- [5] M. S. van Buijtenen, W. J. van Dijk, N. G. Deen, J. A.M. Kuipers, T. Leadbeater, D. J. Parker, Numerical and experimental study on multiple-spout fluidized beds. *Chemical Engineering Science* **66**, 2368-2376 (2011). <https://doi.org/10.1016/j.ces.2011.02.055>
- [6] B. Esgandari, S. Golshan, R. Zarghami, R. Sotudeh-Gharebagh, J. Chaouki, CFD-DEM analysis of the spouted fluidized bed with non-spherical particles. *The Canadian Journal of Chemical Engineering* **99**, 2303-2319 (2021). <https://doi.org/10.1002/cjce.24142>
- [7] T. Weinhart, R. Hartkamp, A. R. Thornton, S. Luding, Coarse-grained local and objective continuum description of three-dimensional granular flows down an inclined surface. *Physics of Fluids* **25**, 070605 (2013). <https://doi.org/10.1063/1.4812809>
- [8] B. Füvesi, C. Goniva, S. Luding, V. Magnanimo, Mixing indices in up-scaled simulations. *Powder Technology* **456**, 120775 (2025). <https://doi.org/10.1016/j.powtec.2025.120775>
- [9] Y. Zhang, B. Jin, W. Zhong, Experiment on particle mixing in flat-bottom spout-fluid bed. *Chemical Engineering and Processing* **48**, 126-134 (2009). <https://doi.org/10.1016/j.ccep.2008.02.012>